

Open Charm and Beauty Production at HERA

Karin Daum^{*1}

**Rechenzentrum, Universität Wuppertal
Gaußstraße 20, D-42097 Wuppertal, Germany*

Abstract.

Measurements on open charm and beauty production in ep collisions at a center-of-mass energy of $\sqrt{s} = 300$ GeV performed by the H1 experiment at HERA are presented. Final states containing charm are identified by the reconstruction of $D^{*\pm}$ meson while events containing muons and at least two jets were used to select data samples enriched with beauty. The results cover the region of negative four-momentum transfer squared Q^2 from photoproduction ($Q^2 \approx 0$) to deep inelastic scattering at large Q^2 . The experimental results are compared with QCD predictions.

INTRODUCTION

The study of heavy flavor production in lepton-proton scattering provides an important tool for testing the standard model of strong interactions. At the ep collider HERA, which was operated at a center-of-mass energy of $\sqrt{s} = 300$ GeV, heavy quarks are almost exclusively produced by the *photon gluon fusion (PGF)* process, $\gamma g \rightarrow Q\bar{Q}$ ($Q = c, b$), where a real or virtual photon emitted by the electron² interacts with a gluon in the proton producing a heavy quark pair $Q\bar{Q}$.

The dominant contribution to heavy flavor production is due to the exchange of an almost real photon (*photoproduction*), where the negative square of the four-momentum transfer carried by the photon is ($Q^2 \approx 0$). The heavy quarks hadronize and may be detected as "*open charm (beauty)*", i.e. with charmed/beauty hadrons visible in the final state.

The kinematics of the ep interaction is described by three independent variables, the center-of-mass energy \sqrt{s} , the four-momentum transfer squared of the photon $q^2 = -Q^2$ and either one of the scaling variables $y = (q \cdot P)/(l \cdot P)$, the inelasticity of the ep interaction, or Bjorken- x $x = Q^2/(2P \cdot l)$. Here P and l denote the four-momentum of the proton and the electron, respectively. The γp center-of-mass energy squared is given by $W_{\gamma p}^2 = W^2 \approx y \cdot s - Q^2$.

¹⁾ permanent at DESY, Notkestraße 85, D-22607 Hamburg, Germany, email: daum@mail.desy.de

²⁾ Hereafter, a reference to electrons implies a reference to either electrons or positrons.

Open heavy flavor production at HERA is dominated by charm production. The analysis of these data starts to allow detailed testing of perturbative QCD (*pQCD*) because of the high luminosity delivered by HERA in recent years. Due to the large mass m_b and the charge of beauty quarks the cross section for $\sigma(ep \rightarrow eb\bar{b}X)$ is expected to be roughly two orders of magnitude smaller than $\sigma(ep \rightarrow ec\bar{c}X)$. Despite of this, the study of beauty production in lepton nucleon scattering is of special interest because the calculations in pQCD are expected to be more reliable due to the large scale, i.e. m_b , involved in this process.

The results presented here [1-3] are based on roughly 19 pb^{-1} of data recorded by H1 [4] in 1996 and 1997 at HERA, when positrons with an energy of 27.5 GeV were collided head-on protons of 820 GeV.

OPEN HEAVY FLAVOR PRODUCTION

The description of open heavy flavor production is based on pQCD. In leading order (LO) the *direct* photon gluon fusion process ($\gamma g \rightarrow Q\bar{Q}$) is the dominant contribution. In photoproduction (γp) sizable contributions from *resolved* photon interactions, i.e. $gg \rightarrow Q\bar{Q}$, are expected due to the partonic structure of the photon. In next-to-leading order (NLO) or beyond, however, the resolved photon processes are part of the higher order contributions and the distinction between direct and resolved processes becomes impossible.

NLO Calculation in the DGLAP Scheme

Several schemes are used to perform NLO calculations. All approaches assume the scale to be hard enough to apply pQCD and to guarantee the validity of the factorization theorem.

Here, the massive approach is adopted which is a fixed order calculation (in α_s) with massive quarks, i.e. $m_Q \neq 0$, assuming three active flavors in the proton. The densities of the three light quarks and the gluon in the proton and the photon are obtained by the DGLAP evolution. Heavy quark are produced perturbatively [5,6] via boson gluon fusion. These calculations are reliable near threshold, where for the renormalization scale μ the relation $\mu^2 \approx m_Q^2$ is valid. However, they break down for $\mu^2 \gg m_Q^2$ due to large logarithms $\ln(\mu^2/m_Q^2)$. Based on the NLO calculations of order α_s^2 in the coefficient functions [7,8] the Monte Carlo integration program HVQDIS [9] and the FMNR code [10] provides the four-momenta of the outgoing partons in the DIS and the γp regime, respectively. Thus the calculation of visible differential inclusive heavy meson production cross sections becomes possible.

The heavy flavored quarks are fragmented to heavy flavored mesons according to the longitudinal Peterson fragmentation function [11], which is controlled by a single parameter ϵ . In the analysis of open charm production the D^{*+} meson is given a transverse momentum p_t with respect to the charm quark in addition, according to

the function $\exp(-\alpha p_t^2)$, to account for the experimentally observed p_t smearing of hadrons with respect to the quark direction. The parameter α is chosen such that an average transverse momentum $\langle p_t \rangle \approx 350$ MeV is obtained as observed in e^+e^- data. In the analysis open beauty production both, the longitudinal fragmentation model and a more complex modeling of the fragmentation process by picking up light quark pairs from the vacuum has been used. Finally, the weak decay of beauty hadrons into muons is included.

CCFM Evolution

The results of the open charm production in DIS will also be compared with predictions based on the CCFM evolution equation [12]. This evolution scheme may be most appropriate to describe the parton evolution at small x . In the parton cascade, gluons are emitted in an angular ordered region to account for coherence effects. Due to this ordering, the unintegrated gluon distribution in CCFM depends on the maximum allowed angle in addition to the momentum fraction x and the transverse momentum of the propagator gluon. The cross section is then calculated according to the k_t -factorization theorem by convoluting the unintegrated gluon density with the off-shell boson gluon fusion matrix element with massive quarks for the hard scattering process, well suited for heavy flavor production.

Based on a recent solution of the CCFM equation [13] a full hadron level Monte Carlo generator CASCADE has been developed [14] in which the full generation of charm events, including the initial state gluon radiation according to CCFM and Lund string fragmentation (JETSET) is also possible. The fragmentation of charmed quarks to $D^{*\pm}$ mesons is performed using the Peterson fragmentation function $\epsilon = 0.078$. A refined version of CASCADE with the unintegrated gluon density [15] as extracted from the H1 F_2 data [16] has been used.

OPEN CHARM PRODUCTION IN DIS

Open charm production is tagged by the observation of $D^{*\pm}$ in the final state. $D^{*\pm}$ mesons are identified by the decay chain $D^{*\pm} \rightarrow D^0 \pi^\pm$, $D^0 \rightarrow K^\mp \pi^\pm$ in the visible range of the transverse momentum $p_\perp(D^*) > 1.5$ GeV and the pseudorapidity $|\eta(D^*)| < 1.5$ in the laboratory frame, where the pseudorapidity is defined as $\eta(D^{*\pm}) = -\ln \tan(\Theta_{D^{*\pm}}/2)$. For the DIS selection the event kinematics is restricted to $0.05 < y < 0.7$ and $2 \text{ GeV}^1 < Q^2 < 100 \text{ GeV}^2$.

In figure 1 the inclusive single differential $D^{*\pm}$ cross sections in the visible region are shown as a function of the kinematic quantities W , x_{Bj} and Q^2 and as a function of the D^{*+} observables $p_t(D^*)$, $\eta(D^*)$ and $z_D(D^*) = P \cdot p_{D^*} / P \cdot q$, where P , q and p_{D^*} denote the four-momenta of the incoming proton, the exchanged photon and the observed $D^{*\pm}$. Also shown in Fig.1 are the expectations from the NLO calculations of the HVQDIS program using the GRV 98 HO parton density parameterization [17]. The dark shaded band indicates the uncertainties in this calculation by varying

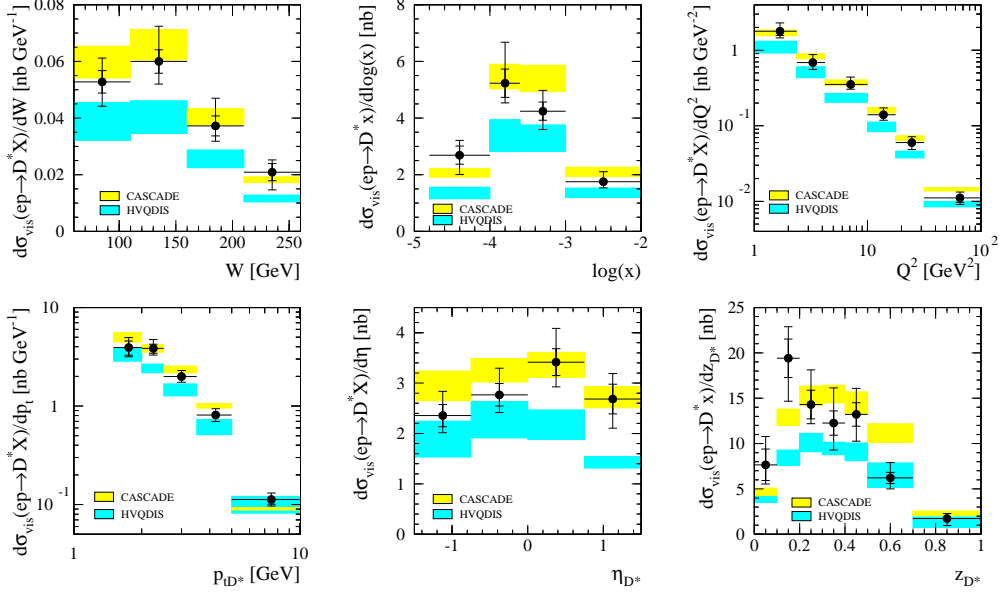


FIGURE 1. Single differential inclusive cross section $\sigma(ep \rightarrow eD^{*+}X)$ versus W , x_{Bj} , Q^2 and $p_{T D^*}$, η_{D^*} , z_{D^*} . The NLO DGLAP expectation (HVQDIS) is indicated by the lower shaded band (upper bounds: $m_c = 1.3$ GeV, $\epsilon = 0.035$, lower bounds: $m_c = 1.5$ GeV, $\epsilon = 0.10$). The upper shaded band is the CCFM expectation (CASCADE) (1.3 GeV $< m_c < 1.5$ GeV, $\epsilon = 0.078$).

m_c and ϵ from $m_c = 1.3$ GeV and $\epsilon = 0.035$ (upper limit) to $m_c = 1.5$ GeV and $\epsilon = 0.10$ (lower limit). The renormalization scale and the factorization scale are set to $\mu_r^2 = \mu_f^2 = Q^2 + 4m_c^2$. Although the total visible cross section prediction of HVQDIS is smaller than experimentally observed, the agreement with the data in the shapes of the different single differential cross sections is reasonable. A difference in shape is observed only in the $d\sigma/d\eta$ cross section. In the forward direction, the observed D^{*+} meson production cross section is considerably larger than predicted by this calculation. This excess is also manifest in the larger cross section observed in the data at small z_D .

Figure 1 also includes the predictions of the CCFM calculations using the CASCADE program (light shaded band) with varying m_c between 1.3 GeV and 1.5 GeV and using $\epsilon = 0.078$. The expectations from the CASCADE program are found to agree better with data in general and especially in the forward η region, where the HVQDIS program fails to describe the data. It is interesting to note that the CCFM calculation, which starts from completely different principles and aims specifically to describe low x phenomena, is able to describe open charm production at HERA better than the DGLAP based NLO calculations with the chosen settings.

The charm contribution $F_2^c(x, Q^2)$ to the proton structure function is obtained by using the expression for the one photon exchange cross section for charm production

$$\frac{d^2\sigma^c}{dx dQ^2} = \frac{2\pi\alpha^2}{Q^4 x} \left(1 + (1-y)^2\right) F_2^c(x, Q^2). \quad (1)$$

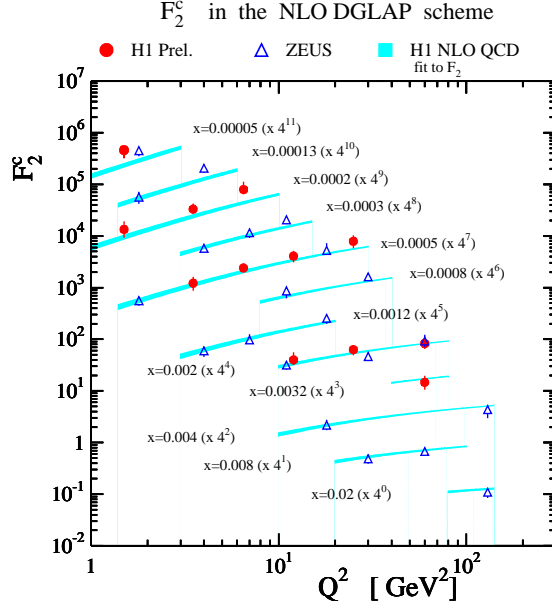


FIGURE 2. The charm contribution to the proton structure function F_2^c as derived from the inclusive D^{*+} meson as a function of Q^2 for different bins in x . The error bars refer to the statistical (inner) and the total error (outer), respectively. The shaded bands represent the predictions of the NLO DGLAP evolution based on the parton densities in the proton obtained by the NLO fit to the inclusive F_2 .

The range of y of the measurements is such that contribution from the second structure function F_1 is everywhere negligible.

The visible inclusive D^{*+} cross sections $\sigma_{\text{vis}}^{\text{exp}}(x, Q^2)$ in bins of x and Q^2 are converted to a bin center corrected $F_2^c \text{ exp}(\langle x \rangle, \langle Q^2 \rangle)$ by the relation:

$$F_2^c \text{ exp}(\langle x \rangle, \langle Q^2 \rangle) = \frac{\sigma_{\text{vis}}^{\text{exp}}(x, Q^2)}{\sigma_{\text{vis}}^{\text{theo}}(x, Q^2)} \cdot F_2^c \text{ theo}(\langle x \rangle, \langle Q^2 \rangle), \quad (2)$$

where $\sigma_{\text{vis}}^{\text{theo}}$ and $F_2^c \text{ theo}$ are the theoretical predictions of HVQDIS.

In Fig. 2 the charm contribution to the proton structure function F_2^c is shown as a function of Q^2 for different bins in x in the NLO DGLAP picture together with the results from ZEUS [19]. Also shown is the expectation using the result on the gluon density from the H1 NLO DGLAP fit to the inclusive F_2 measurement [20]. The band indicates the uncertainty in this extraction introduced by varying the charm quark mass between 1.3 GeV and 1.5 GeV. Other sources of uncertainties in the determination of the gluon density in the proton are not yet taken into account. The charm data show large scaling violations visible in the variation of F_2^c with Q^2 for constant x_{Bj} . The amount of scaling violation present in the charm data is well predicted by the NLO DGLAP evolution on the gluon density extracted from the inclusive F_2 measurement.

OPEN BEAUTY IN PHOTOPRODUCTION

Two independent analyses of open beauty photoproduction [2,3] have been performed by H1. Based on data from different years they make use of different features of beauty hadron decays for tagging. Both analysis are based on the semileptonic decay of beauty hadrons resulting in muons identified in the final state. The muon has to be observed in the central region of the detector, i.e. $35^\circ < \theta^\mu < 130^\circ$, and its transverse momentum p_\perp^μ has to exceed 2 GeV. In addition, at least two high E_\perp^{jet} jets have to be found in the events. At least one of the jets has to contain a muon candidate fulfilling the requirements above. The γp -regime is defined by requiring that no electron candidate is observed with $\theta_e < 177.8^\circ$, which limits the data samples to $Q^2 < 1 \text{ GeV}^2$.

Large Mass Tagging

The analysis of the 1996 data [2] makes use of the fact that b quarks are much heavier than c quarks for a statistical separation of b and c events. In contrast to charmed hadrons the decay products of beauty hadrons are expected to show large transverse momenta $p_{T,rel}$ with respect to the direction flight of the decaying beauty hadron. Since this analysis does not attempt to reconstruct the beauty hadron directly its direction is approximated by the thrust axis of the jet containing the muon. In this analysis the optimal distinction of charm and beauty events is expected if the $p_{T,rel}^\mu$ of the muon is considered.

Apart from semileptonic charm and beauty decays other hadrons do contribute to the muon sample because of misidentification. The misidentification probabilities for pions, kaons and protons have been parameterized using Monte Carlo simulations. They are verified by studying K_s^0 and ϕ decays in data, which present unambiguous sources of pions and kaons, respectively.

In figure 3 the measured $p_{T,rel}^\mu$ distributions is shown together with the fitted contributions of beauty and charm, using the shapes from AROMA Monte Carlo simulations, and the hadronic background determined from the data. The data exhibits a significant tail to large $p_{T,rel}^\mu$ values. As expected the $p_{T,rel}^\mu$ distribution in b events is significantly harder than in c events, while the distribution of the hadronic background is similar in shape to expectation from semileptonic charm decay.

The visible electroproduction cross section of b quarks, determined from the number of muons N_b^μ attributed to b quark decays, is measured to be:

$$\sigma_{vis}(ep \rightarrow ebb\bar{X} \rightarrow \mu X) = 176 \pm 16(stat.)_{-17}^{+26}(syst.)pb$$

in the kinematic range $Q^2 < 1 \text{ GeV}^2$, $0.1 < y < 0.8$, $p_\perp^\mu > 2 \text{ GeV}$ and $35^\circ < \theta^\mu < 130^\circ$.

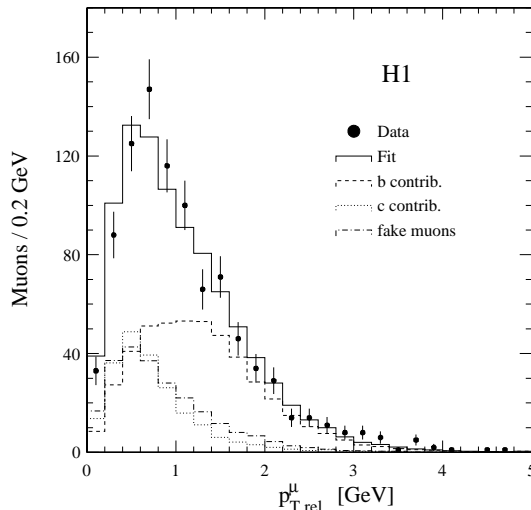


FIGURE 3. The measured $p_{T,rel}^{\mu}$ distribution in the data and the fitted sum (solid line) of the contribution of beauty (dashed line), charm (dotted line) and the fixed fake muon background (dashed dotted line).

Lifetime Tagging

The second analysis [3] makes use of the longevity of b mesons. This only became possible since 1997 when the central silicon tracker (CST) [4] of H1 was fully commissioned. For each muon candidate the impact parameter δ is calculated in the plane perpendicular to the beam axis. Its magnitude is given by the distance of closest approach of the track. Its sign is positive if the intercept of the track with the jet axis is downstream of the primary vertex, and negative otherwise. Decays of long-living particles are expected to have large positive impact parameters, whereas particles from the primary vertex should yield a symmetric distribution around zero due to resolution effects.

Figure 4a shows the observed impact parameter distribution for the data together with histograms indicating the contribution from b productions and from the backgrounds. The decomposition is obtained from a likelihood fit. The fit uses the shapes of the δ distribution of b and c events from the AROMA Monte Carlo simulation and the fake muon events from real data. The observed δ distribution clearly shows a tail to large positive values, which indicates a sizable contribution of b events in the data.

The data taken in 1997 also enables the measurement of both, δ and $p_{T,rel}^{\mu}$ simultaneously for the events. By imposing a cut on one of these two variables it is possible to further enrich the b component while studying the distribution of the other quantity. Figures 4b and 4c shows the observed δ distribution while cutting in $p_{T,rel}^{\mu}$ and vice versa together with the predictions obtained by the fit to the distribution of Figure 4a. A good description of the data is observed in these restricted areas of phase space where the b contribution clearly dominates. Therefore, a fit in

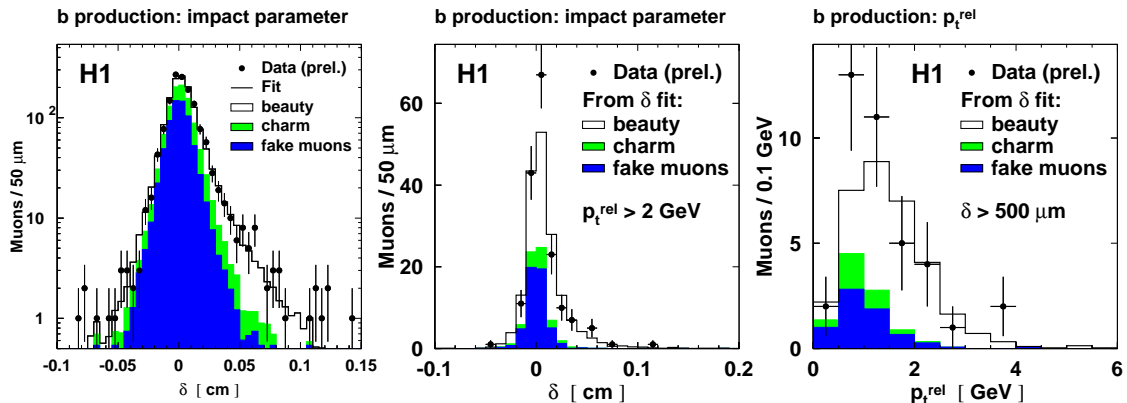


FIGURE 4. Results from the impact parameter analysis: the measured δ distribution (a) for all selected muon events and its decomposition from the likelihood fit, and (b) for those events having a muon with $p_{T,rel}^\mu > 2$ GeV, and the observed $p_{T,rel}^\mu$ distribution for events having muons with $\delta > 500\mu\text{m}$.

the δ - $p_{T,rel}^\mu$ plane is performed, which leads to a cross section of

$$\sigma_{vis}(ep \rightarrow ebb\bar{X} \rightarrow \mu X) = 160 \pm 16(stat.) \pm 29(syst.) \text{ pb}$$

in the kinematic range $Q^2 < 1 \text{ GeV}^2$, $0.1 < y < 0.8$, $p_{\perp}^\mu > 2 \text{ GeV}$ and $35^\circ < \theta^\mu < 130^\circ$, agreeing well with the measurement based on the 1996 data. Taking into account correlated systematics the combination of both measurement yields to

$$\sigma_{vis}(ep \rightarrow ebb\bar{X} \rightarrow \mu X) = 170 \pm 22 \text{ pb.}$$

NLO pQCD predicts $(104 \pm 17)\text{pb}$ [2], using the FMNR program [10] together with a Peterson type fragmentation, where the error reflects the uncertainties due to variations in the renormalization or factorization scale, and to fragmentation. This value is significantly smaller than observation. Such a discrepancy is now established in both ep and $p\bar{p}$ interactions [21].

CONCLUSIONS

New results on differential inclusive D^{*+} meson production cross sections in deep inelastic ep scattering from the 1996 and 1997 H1 data have been presented. These measurements favor the predictions of the CCFM based CASCADE program over those of the NLO DGLAP based HVQDIS program in terms of the parameter space explored in the current analysis. By extrapolating the visible D^{*+} meson production cross section to full phase space in $p_t(D^{*+})$ and $\eta(D^{*+})$, the charm contribution to the proton structure F_2^c has been extracted. The data show large scaling violations.

Two independent analysis using data from different years and different tagging techniques have shown that the open beauty photoproduction cross section in ep scattering at HERA is significantly above NLO pQCD expectation.

REFERENCES

1. C. Adloff *et al.* (H1 Collab.), Contributed paper to the 30th International Conference on High-Energy Physics ICHEP2000, Osaka, Japan, July 2000, abstract, 984.
2. C. Adloff *et al.* (H1 Collab.), *Phys. Lett.* **B 467**, 156 (1999).
3. C. Adloff *et al.* (H1 Collab.), Contributed paper to the 30th International Conference on High-Energy Physics ICHEP2000, Osaka, Japan, July 2000, abstract, 979,982.
4. I. Abt *et al.* (H1 Collab.), *Nucl. Inst. Meth.* **A 386**, 310 and 348 (1997).
5. E. Laenen *et al.*, *Nucl. Phys.* **B 392** 162,229 (1993), *Nucl. Phys.* **B 291** 325 (1992); S. Riemersma, J. Smith, and W.L. van Neerven: *Phys. Lett.* **B 347** 142 (1995).
6. S. Frixione *et al.*, *Phys. Lett.* **B 348** 633 (1995).
7. B.W. Harris and J. Smith, *Nucl. Phys.* **B 452** 109 (1995), *Phys. Lett.* **B 353** 535 (1995).
8. R.K. Ellis and P. Nason, *Nucl. Phys.* **B 312** 551 (1989); P. Nason, S. Dawson and R.K. Ellis, *Nucl. Phys.* **B 303** 607 (1988), *Nucl. Phys.* **B 327** 49 (1989).
9. B.W. Harris and J. Smith, *Phys. Rev.* **D 57** 2806 (1998).
10. M.L. Mangano, P. Nason and G. Ridolfi, *Nucl. Phys.* **B 373** 295 (1992); S. Frixione *et al.* *Nucl. Phys.* **B 412** 225 (1994).
11. C. Peterson *et al.*, *Phys. Rev.* **D 27** 105 (1983).
12. M. Ciafaloni, *Nucl. Phys.* **B 296** 49 (1988); S. Catani, F. Fiorani and G. Marchesini, *Phys. Lett.* **B 234** 339 (1990), *Nucl. Phys.* **B 336** 18 (1990); G. Marchesini, *Nucl. Phys.* **B 445** 45 (1995).
13. H. Jung, Proc. 7th DIS Workshop, *Nucl. Phys.* **B 79** 429 (1999) (Proc. Suppl.), hep-ph/9905554.
14. H. Jung, Proc. Workshop on Monte Carlo Generators for HERA Physics, 1999, DESY-PROC-1999-02, p.75, hep-ph/9908497; H. Jung and G. Salam, to be published.
15. S.P. Baranov, H. Jung and N.P. Zotov, Proc. Workshop on Monte Carlo Generators for HERA Physics, 1999, DESY-PROC-1999-02, p.484.
16. S. Aid *et al.* (H1 Collab.), *Nucl. Phys.* **B 470** 3 (1996).
17. M. Glück, E. Reya and A. Vogt, *Eur. Phys. J.* **C 5** 461 (1998).
18. C. Adloff *et al.* (H1 Collab.), *Z. Phys.* **C 72** 593 (1996).
19. J. Breitweg *et al.* (ZEUS Collab.), *Phys. Lett.* **B 407** 402 (1997) 402, *Euro. Phys. J.* **C 12** 1 (2000).
20. C. Adloff *et al.* (H1 Collab.), Contributed paper to the 30th International Conference on High-Energy Physics ICHEP2000, Osaka, Japan, July 2000 abstract 945
21. F. Abe *et al.* (CDF Collab.), *Phys. Rev. Lett.* **71** 2396 (1993), *Phys. Rev.* **D 53** 1051 (1996); S. Abachi *et al.* (D0 Collab.) *Phys. Rev. Lett.* **74** 3548 (1995), *Phys. Lett.* **B 370** 239 (1996).